Available online at www.sciencedirect.com

SciVerse ScienceDirect

Ceramics International 38 (2012) 4573–4578

CERAMICS INTERNATIONAL

www.elsevier.com/locate/ceramint

Influence of TiO_2 on the physical properties of low-temperature ceramic vitrified bond and mechanical properties of CBN composites

Dongdong Shan, Zhihong Li, Yumei Zhu *, Hang Ye, Kai Gao, Yanyan Yu

Key Laboratory for Advanced Ceramics and Machining Technology of Ministry of Education, School of Materials Science and Engineering, Tianjin University, Tianjin 300072, People's Republic of China

Received 13 September 2011; received in revised form 17 January 2012; accepted 13 February 2012
Available online 21 February 2012

Abstract

The microstructures and properties of vitrified bond abrasive tools made of CBN grains and advanced vitrified bond systems with different TiO_2 doping amounts were investigated. Based on the experimental observations and analysis, the incorporation of TiO_2 in appropriate amount (4 wt.%) was beneficial to the improvement on flowing ability and thermal expansion property of the vitrified bond systems, and mechanical properties of the CBN composites including bending strength and Rockwell hardness were obviously improved. On the basis of discussion for microstructure, the CBN grains were better covered by vitrified bond and acquired less pores when the content of TiO_2 reached 4 wt.%. These results were related to the role of TiO_2 in the glass network structure which was analyzed by Fourier transform infrared spectroscopy (FTIR).

Keywords: C. Mechanical properties; Vitrified bond; CBN composites; TiO_2 doping; Microstructures

1. Introduction

CBN abrasive tools are a group of high performance superhard composite materials with excellent abrasion resistance, good thermal conductivity, etc. Owing to the excellent properties, CBN grinding tools are becoming one of the most potential tools in modern engineering applications [1,2]. Besides the characteristics of abrasive themselves, the mechanical properties of grinding tools mainly depend on the performance of bond systems and combination state between bond systems and abrasives.

Among four types of bond systems applied to fix abrasive grains into the grinding wheels, i.e., metallic, resinous, electro-plated and vitreous bond, the last one was considered as one of the most important systems [3–6]. In comparison with other types of grinding tools, vitrified bond grinding tools show outstanding properties on account of excellent properties of the vitrified bond materials, such as high elastic modulus, low fracture toughness, good thermal stability, brittle, high rigidity and controllable porosity [7]. However, the development of vitrified bond systems for CBN abrasives cannot well balance the requirement of grinding performance, wheel safety, and product consistency [8], thus, bond properties should be improved to take full advantage of the operational properties of abrasive grains. As a consequence, investigations on the improvement of vitrified bond properties should be carried out.

Previous studies have investigated the influences of different additives (CaO, ZnO, alkali oxides, etc.) and their content on the mechanical properties and microstructures of vitrified bond CBN/corundum/diamond grinding tools [9–12]. And the effects of different raw materials introduced into vitrified bond for CBN/corundum grinding wheels have been also reported in some literatures [13,14]. Referring to vitrified bond for grinding tools with the addition of different amounts of TiO_2, relevant works have not been published.

In this paper, SiO_2–B_2O_3–Na_2O–BaO vitrified bond systems with and without TiO_2 were prepared, and vitrified bond CBN composites were made as well. We had investigated the combination state between vitrified bond and CBN grains by means of scanning electron microscope (SEM) and the micro-scale bonding mechanism of vitrified bond by Fourier transform infrared spectroscopy (FTIR). The bending strength, Rockwell hardness of grinding tools were also characterized.

* Corresponding author. Tel.: +86 022 27404260; fax: +86 022 27404260.
E-mail address: linzhongyudi@126.com (Y. Zhu).

0272-8842/$36.00
doi:10.1016/j.ceramint.2012.02.035

2. Experimental procedure

2.1. Preparation of vitrified bond and CBN composites

The basic vitrified bond consisting of silica, alumina, boron oxide, sodium oxide, potassium oxide, barium oxide. The mass percentage was 50 wt.%, 12 wt.%, 19 wt.%, 7 wt.%, 7 wt.%, and 5 wt.%. They were introduced in the form of silica, alumina, boric acid, sodium carbonate, potassium carbonate, barium carbonate, etc. TiO_2 was added in the content of 4 wt.% and 8 wt.%, respectively. After accurate weighing, mixing, ball milling and melting in the alumina crucibles at 1300 °C, the basic vitrified bond and the vitrified bond with TiO_2 in amorphous status had been prepared. Vitrified bond powder had been acquired after screening (240#). The specimens of vitrified bond with 0 wt.% TiO_2, 4 wt.% TiO_2 and 8 wt.% TiO_2 were signed as A, B, C in this work.

After screened and molded into rectangular bars (30 mm × 6 mm × 4 mm) by dry pressing, the CBN composites made of CBN grains (monocrystal, average grain size 140#, Henan Funik Ultrahard Material Co. Ltd., China), temporary binder (wax), vitrified bond with and without TiO_2 were sintered in the electric furnace in air at different sintering temperatures (720 °C, 740 °C, 760 °C, 780 °C, 800 °C). The holding time of these specimens were 2 h.

2.2. Characterizations of vitrified bond and the combination state with CBN grains

Binding state between vitrified bond and CBN grains is a critical problem for CBN composites. Fluidity applied to evaluate the bonding state of vitrified bond systems to abrasive grains was measured by plane flowing method (after the bond powders molded to cylinders, the specimens are put on the ceramics plate and sintered in the furnace, then the change of the diameters can be measured and the fluidity can be calculated). Thermal expansion coefficient was performed by the apparatus of NETZSCH DIL402C (Germany). Mechanical properties were characterized by bending strength and Rockwell hardness. The bending strength was measured by using three-point bending method according to C158ASTM in MTS machine at a cross-head speed of 0.6 mm/min. The Rockwell hardness was performed by the instrument of HR-150A. Microstructures of the fracture surfaces of sintered composites were evaluated by scanning electron microscope (Phillips XL30). The Fourier transform infrared spectroscopy (FTIR) measurements were carried out on an instrument of Nicollet FT-IR 470 with the wavenumber range of 400–4400 cm^{-1} (vitrified bond powders were dispersed in KBr pellets (3 wt.%)).

3. Results and discussions

3.1. Flowing ability and thermal expansion coefficients of vitrified bond

Fluidity and thermal expansion coefficient are the most widely used parameters for estimating the flowing ability and thermal expansion property of vitrified bond. Outstanding flowing ability and thermal expansion property of vitrified bond to abrasives have great influence on the interface status between the bonds and the abrasive grains.

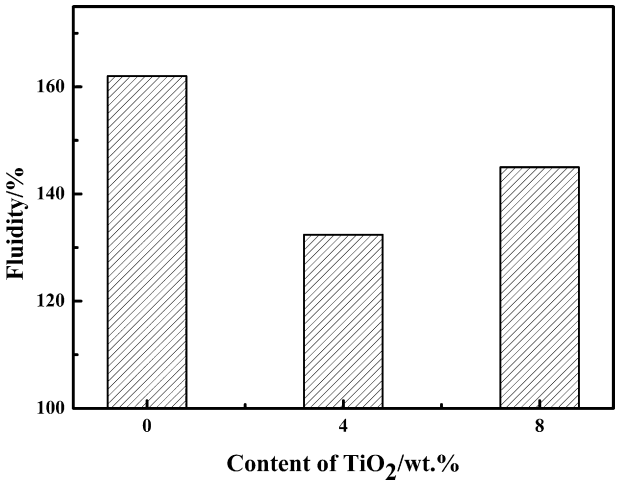

Fig. 1. Influence of TiO_2 content on the fluidity of vitrified bond systems.

In this part of our experiments, the sintering temperature was scheduled to be 780 °C for grinding wheels with vitrified bond A, B and C. Fig. 1 shows the variation of fluidity (three values take average) for vitrified bond A, B and C at the sintering temperature of 780 °C. And the thermal expansion coefficients for vitrified bond with different TiO_2 doping amounts at the sintering temperature of 780 °C were shown in Fig. 2.

As shown in Fig. 1, the fluidity of the TiO_2 doped vitrified bond was lower than that of the basic vitrified bond. The fluidity of vitrified bond A was 162%, about 30% higher than that of vitrified bond B. When the content of TiO_2 reached 8 wt.%, the fluidity of vitrified bond C was about 10% higher than that of vitrified bond B. In Fig. 2, we could see that the average value of the thermal expansion coefficient for vitrified bond A (6.835×10^{-6} °C^{-1}) from the initial temperature to the soft point was higher than that for vitrified bond B (5.165×10^{-6} °C^{-1}) and C (6.29×10^{-6} °C^{-1}).

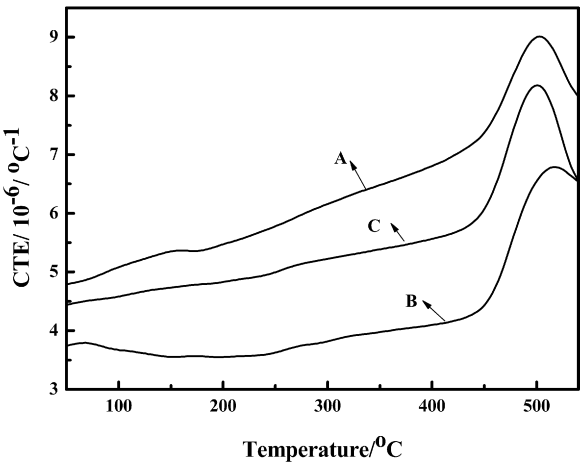

Fig. 2. Thermal expansion coefficients of vitrified bond with different TiO_2 doping amounts.

It should be believed that the differences of fluidity and thermal expansion coefficients might resulted from the formation of different network structure of the vitrified bond. Titanium ions existed in the [TiO_4] tetrahedrons acting as network former and [TiO_6] octahedrons as network modifier. TiO_2 would be normally expected to have a coordination number of six as a consequence of the high field strength of titanium ions (0.68 Å). But in order to be a part of the glass network structure and compatible with the silicate network at high temperature, some of titanium ions might have a coordination number of four. The [TiO_4] tetrahedrons enhanced the glass formation ability without inducing the formation of any non-bridging oxygen ions [15–17]. Therefore, titanium ions in the glass existed mainly in the form of [TiO_4] tetrahedrons. However, when the content of TiO_2 increased to some certain values, some [TiO_4] tetrahedrons had the tendency to change to [TiO_6] octahedrons. Although [TiO_6] octahedrons acted as network modifier, titanium ions filled into the space of glass network also had some positive effect on the densification of the glass network structure. Based on the analysis above, the thermal expansion coefficients decreased due to the densification of the glass network structure. And the viscosity of the vitrified bond related to the densification of internal network would increased first and had a decreasing tendency then, thus, the fluidity which had inverse proportion to viscosity got opposite variation.

3.2. Bending strength and Rockwell hardness of CBN composites

Bending strength and Rockwell hardness are parameters used to characterize the mechanical properties of the grinding tools. The values are closely related to the strength of vitrified bond and the combination state between vitrified bond and abrasive grains. The samples with higher bending strength always own higher Rockwell hardness.

Bending strength (Five values take average) of CBN composites with different vitrified bond sintering at different temperatures could be seen in Fig. 3. As shown in Fig. 3, the bending strength of vitrified bond specimens showed similar tendency. Firstly, they got remarkably increased as the sintering temperatures increased in a certain extent, and then decreased when the sintering temperatures exceeded optimal temperature (optimal temperature was 780 °C in this experiment). The flowing ability of vitrified bond leading to better combination state between vitrified bond and abrasive grains were improved with the increase of sintering temperatures, consequently, the bending strength enhanced as well. However, when surpassed optimal temperature, the specimens would be over-sintered, inducing distortion and foaming of the specimens, simultaneously, the strength of the specimens decreased.

It also could be seen from Fig. 3 that the bending strength of the specimens with vitrified bond B (57.3 MPa) at the optimal sintering temperature was much higher than that with vitrified bond A (49 MPa). Nevertheless, when the concentration of TiO_2 reached 8 wt.%, the bending strength of the specimens (53.7 MPa) at the optimal sintering temperature decreased but still higher than that of the specimens with vitrified bond A.

Rockwell hardness (five values take average) of CBN composites with different vitrified bond sintering at optimal temperature (780 °C) were shown in Fig. 4. It could be seen that the Rockwell hardness of the specimens with vitrified bond B (63.1 HRB) was much higher than that with vitrified bond A (55.1 HRB). However, when the concentration of TiO_2 reached 8 wt.%, the Rockwell hardness of the specimens (57.7 HRB) decreased but still higher than the specimens with vitrified bond A. This result was corresponding to the variation tendency of the bending strength for the specimens.

These results were in harmony with the theory above. Meanwhile it also indicated that the higher fluidity did not mean the better mechanical properties. Matching degree of the thermal expansion coefficients between the vitrified bond systems and CBN grains had significant influence on the mechanical properties of the grinding tools. The thermal expansion coefficients of the vitrified bond systems A, B, C were $6.835 \times 10^{-6}\,°C^{-1}$, $5.165 \times 10^{-6}\,°C^{-1}$ and $6.29 \times 10^{-6}\,°C^{-1}$, respectively. The thermal expansion coefficient for vitrified bond B was closer to CBN than for vitrified

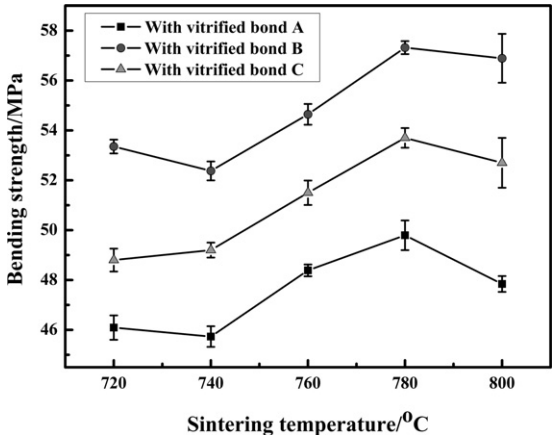

Fig. 3. Effect of TiO_2 content on the bending strength of CBN composites with different sintering temperatures.

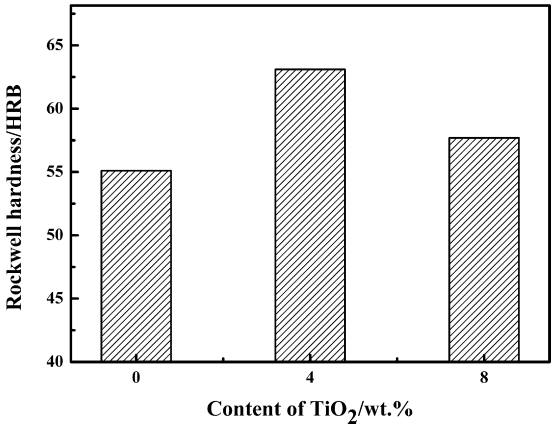

Fig. 4. Rockwell hardness of CBN composites with different TiO_2 doping amounts.

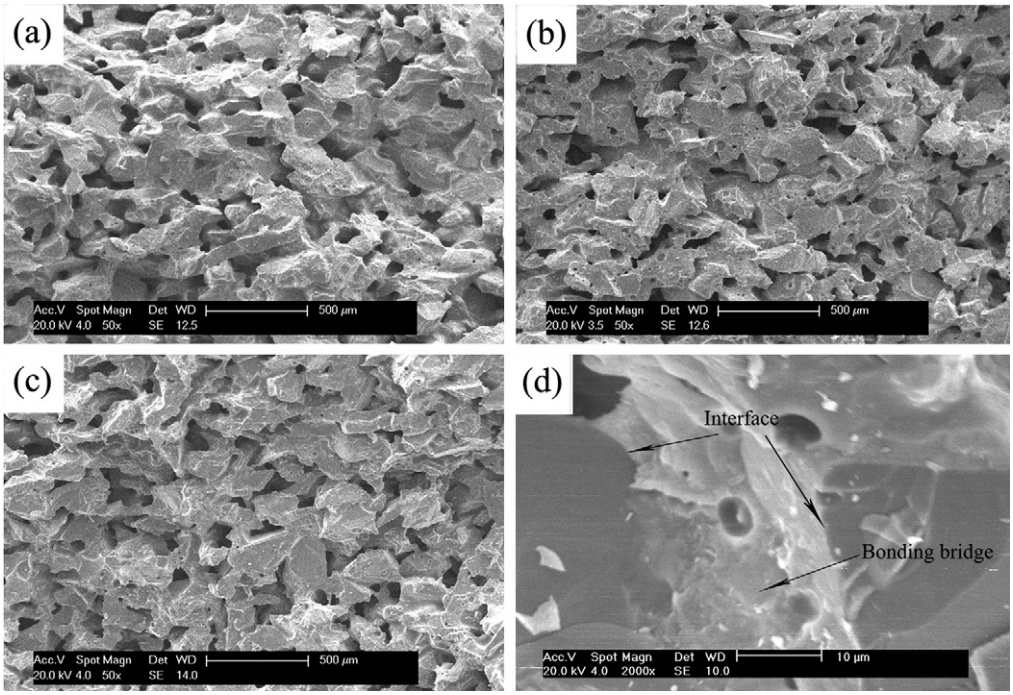

Fig. 5. SEM images of the sintered CBN composites with vitrified bond (a) A; (b) B; (c) C; (d) B (in different amplification factors).

bonds A and C, so the optimal mechanical properties were obtained. In comparison with vitrified bond system A, the thermal expansion coefficient of vitrified bond system C got higher matching degree with CBN grains, thus, the mechanical properties of composites with vitrified bond C was better than that with vitrified bond A. It could be concluded that CBN composites with the vitrified bond B and C (lower than that with vitrified bond B) got higher bending strength and Rockwell hardness than that with vitrified bond A.

3.3. Combination state between vitrified bond systems and CBN grains by SEM analysis

The interfacial state between vitrified bond systems and abrasive grains was shown in Fig. 5. The microstructures of the specimens with different amount of TiO_2 (0 wt.%, 4 wt.%, 8 wt.%) shown in Fig. 5 were significantly different. From Fig. 5a–c, it could be observed that the porosity of the specimens reduced as the TiO_2 was introduced. Compared with the specimens with vitrified bond B and C in Fig. 5b and c, the specimens with vitrified bond A (Fig. 5a) had relatively loosened structure. Comparing to the specimens with vitrified bond C, the abrasive grains were better covered by vitrified bond B, and fewer pores could be observed. The combination state between vitrified bond B and abrasive grains in different amplification factors could be seen in Fig. 5d.

Proper fluidity and thermal expansion coefficient contributed to good mechanical properties and combination state of the specimens. Fluidity lowered to a certain extent could prevent the distortion of the specimens and reduce the amount of pores when TiO_2 was introduced into the basic vitrified bond. The fluidity reduced because of the densification of the glass network structure, but not the more the better. These SEM images demonstrated that the vitrified bond with appropriate content of TiO_2 exhibited excellent combination state to abrasives, consisting with the theory explained above.

3.4. Internal bond analysis by FTIR

Vitrified bond is a solid body with a flexible random structure. Randomness of elements arrangement in glass structure is stabilized by strong polymeric network with covalent-ionic chemical bonds. FTIR analysis is used to estimate the existence of chemical bond vibrating in the amorphous compound.

FTIR spectrums of vitrified bond A, B and C after sintering could be observed in Fig. 6. The three lines were similar in the range of 400–4400 cm^{-1}, the same bands occurred at similar

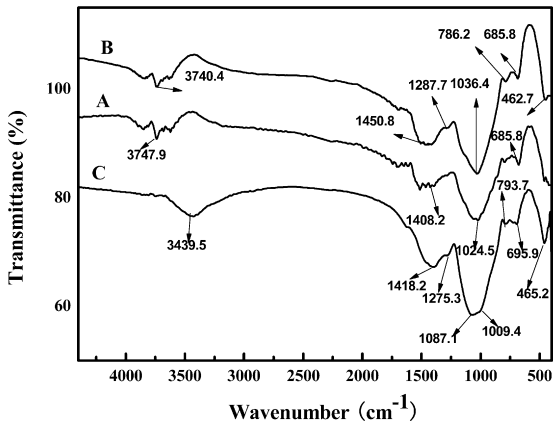

Fig. 6. FTIR spectrums of vitrified bond systems.

wavenumber. Compared with vitrified bond system A, some bands shifting to higher frequency appeared in the curve of vitrified bond system B. The wavenumber shifting also emerged in the curve of vitrified bond system C.

Obvious bands for vitrified bond system A were presented in Fig. 6. The band at about 685.8 cm^{-1} derived from the bending vibration of B–O–B in [BO_3] triangles. The asymmetric stretching vibrations of the Si–O–Si (in [SiO_4] tetrahedrons), B–O–B (in [BO_4] tetrahedrons) and Si–O–B appeared at about 1024.5 cm^{-1}. The positions of stretching vibrations of B–O–B from [BO_3] triangles were at about 1408.2 cm^{-1}. The broad bands between 3000 cm^{-1} and 4000 cm^{-1} were commonly derived from the stretching peaks of hydroxyl group (–O–H). The band at about 3747.9 cm^{-1} was assigned to the absorption band of –O–H. This result was in good agreement with the FTIR features of the glass described in previous studies [18–20].

For vitrified bond system B in Fig. 6, bending vibration of B–O–B (in [BO_3] triangles) still located at 685.8 cm^{-1} with lower intensities than vitrified bond system A. The bands at about 1024.5 cm^{-1} and 1408.2 cm^{-1} belonging to the vibration of silica and boron oxygen polyhedrons shifted to about 1036.4 cm^{-1}, 1450.8 cm^{-1} with strengthened vibration in comparison with vitrified bond system A. Particularly, the obvious bands at about 1287.7 cm^{-1} and 462.7 cm^{-1} from the stretching vibrations of B–O–B (in [BO_3] triangles) and Ti–O–Ti (in [TiO_6] octahedrons) appeared in vitrified bond system B. The titanium framework formed of [TiO_4] tetrahedrons gave bands of stretching and bending vibrations with the wavenumber at about 786.2 cm^{-1}, and the asymmetric stretching vibrations of B–O–Ti as well. The band at about 3740.4 cm^{-1} was also regarded as the characteristic absorption of hydroxyl group. Compared to vitrified bond system B, a small red shift appeared when the content of TiO_2 reached 8 wt.%. The bands located at 462.7 cm^{-1}, 685.8 cm^{-1}, 786.2 cm^{-1}, 1287.7 cm^{-1} and 1450.8 cm^{-1} shifted to 465.2 cm^{-1}, 695.9 cm^{-1}, 1275.3 cm^{-1} and 1418.2 cm^{-1}, respectively. And the band at about 1036.4 cm^{-1} separated into two peaks, 1087.1 cm^{-1} and 1009.4 cm^{-1}, respectively. And the vibration of Ti–O–Ti in [TiO_6] octahedrons was strengthened which indicated that more [TiO_4] tetrahedrons have the tendency of translating to [TiO_6] octahedrons. The band at about 3439.5 cm^{-1} was derived from the absorption band of hydroxyl group [20,21].

The observed differences in wavenumber shifting were attributed to the changes of chemical bonds vibration energy which caused by the densification of glass network. Titanium ions with high coordination number existed in [TiO_4] tetrahedrons and [TiO_6] octahedrons after being introduced into the glass component. Titanium ions in [TiO_4] tetrahedrons were relative with the formation of the glass network, and thus caused the densification of the network structure. Although the conversion of [TiO_4] tetrahedrons to [TiO_6] octahedrons (act as network modifier) occurred during the network forming process when the content of TiO_2 reached a certain value, the glass network could also be strengthened by titanium ions filling the space. Moreover, titanium ions linking with ions of silicon, aluminum and boron by employing the non-bridge oxygen atoms could lessen skeleton broken. Based on the reasons mentioned above, the changing of vibration energy and the shifting of wavenumber to high or low frequency could be well illustrated.

4. Conclusions

The effect of TiO_2 on the microstructures and mechanical properties of SiO_2–B_2O_3–Na_2O–BaO vitrified bond CBN composites were investigated in this work. It had demonstrated that appropriate amount (4 wt.%) of TiO_2 introduced into the SiO_2–B_2O_3–Na_2O–BaO vitrified bond could enhance the bending strength of the specimens from 49 MPa to 57.3 MPa and the Rockwell hardness from 55.1 HRB to 63.1 HRB at optimal sintering temperature (780 °C). The interfacial combination state of the specimens with the vitrified bond containing 4 wt.% TiO_2 was more excellent comparing with other compositions (0 wt.% and 8 wt.%). And the fluidity and thermal expansion properties of vitrified bond which were beneficial to the improvement of combination state between abrasive grains and vitrified bond got the optimal value when the content of TiO_2 reached 4 wt.%.

In FTIR spectrums, the band at about 460 cm^{-1} and 790 cm^{-1} was derived from stretching vibration of Ti–O–Ti in [TiO_6] octahedrons and [TiO_4] tetrahedrons, respectively. The presence of the two structures resulted in the densification of the glass network. Therefore, the results above could be well illustrated.

In conclusion, the introduction of TiO_2 into the basic vitrified bond was beneficial to the properties of CBN composites, but not the more the better.

References

[1] F.C. Gift, W.Z. Misiolek, E. Force, Fluid performance study for groove grinding a nickel-based superalloy using electroplated cubic boron nitride (CBN) grinding wheels, J. Manuf. Sci. Eng. 126 (2004) 451–458.
[2] J.D. Marinescu, W.B. Rowe, B. Dimitro, Tribology of Abrasive Machining Processes, William Andrew Publishing, New York, 2004.
[3] Y. Shang, Y.G. Hou, G.Y. Qiao, W.J. Zou, F.R. Xiao, B. Liao, Effects of nano-AlN on phase transformation of low temperature vitrified bond during sintering process, T. Nonferr. Met. Soc. 19 (2009) 706–710.
[4] D. Herman, J. Krzos, Influence of vitrified bond structure on radial wear of CBN grinding wheels, J. Mater. Process. Technol. 209 (2009) 5377–5386.
[5] H.L. Kuan, T.L. Shun, Influence of vitrified bond structure on radial wear of CBN grinding wheels, Sintering parameters and wear performances of vitrified bond diamond grinding wheels, Int. J. Refract. Met. Hard Mater. 25 (2007) 25–31.
[6] D. Herman, J. Markul, Influence of microstructures of binder and abrasive grain on selected operational properties of ceramic grinding wheels made of alumina, Int. J. Mach. Tools Manuf. 44 (2004) 511–522.
[7] M.J. Jackson, Sintering and vitrification heat treatment of CBN grinding wheels, J. Mater. Process. Technol. 191 (2007) 232–234.
[8] M.J. Jackson, B. Mills, Materials selection applied to vitrified alumina & CBN grinding wheels, J. Mater. Process. Technol. 108 (2000) 114–124.
[9] M.J. Jackson, B. Mills, Interfacial bonding between corundum and glass, J. Mater. Sci. Lett. 19 (2009) 915–917.
[10] M.J. Jackson, N. Barlow, B. Mills, The effect of bond composition on the strength of partially-bonded vitrified ceramic abrasives, J. Mater. Sci. Lett. 13 (1994) 1287–1289.

[11] P.F. Wang, Z.H. Li, J. Li, Y.M. Zhu, Effect of ZnO on the interfacial bonding between Na_2O–B_2O_3–SiO_2 vitrified bond and diamond, Solid State Sci. 11 (2009) 1427–1432.
[12] P.F. Wang, Z.H. Li, Y.M. Zhu, Effect of CaO on the surface morphology and strength of water soaked Na_2O–B_2O_3–Al_2O_3–SiO_2 vitrified bond, J. Non-Cryst. Solids 354 (2008) 3019–3024.
[13] M.J. Jackson, R.T. Wakefield, S.A. Tones, B. Mills, W.B. Rowe, Material selection applied to vitrified corundum grinding wheel, Br. Ceram. Trans. 100 (5) (2001) 229–236.
[14] A.J. Zhang, Z.H. Li, Z.C. Li, Y.M. Zhu, Raw materials selection applied to glass bonding for vitrified CBN grinding wheels, J. Mater. Sci. 43 (2008) 4303–4308.
[15] J. Park, A. Ozturk, Effect of TiO_2 addition on the crystallization and tribological properties of MgO–CaO–SiO_2–P_2O_5–F glasses, Thermochim. Acta 470 (2008) 60–66.
[16] A. Shaim, M. Et-tabirou, Role of titanium in sodium titanophosphate glasses and a model of structural units, Mater. Chem. Phys. 80 (2003) 63–67.
[17] H. Nasu, K. Kurachi, A. Mito, J. Matsuoka, K. Kamiya, Second harmonic generation and structure of mixed alkali titanosilicate glasses, J. Non-Cryst. Solids 217 (1997) 182–188.
[18] L. Stoch, M. Środa, Infrared spectroscopy in the investigation of oxide glasses structure, J. Mol. Struct. 511–512 (511) (1999) 77–80.
[19] K. El-Egili, Infrared studies of Na_2O–B_2O_3–SiO_2 and Al_2O_3–Na_2O–B_2O_3–SiO_2 glasses, Physica B 325 (2003) 340–348.
[20] C.R. Gautam, D. Kumar, O.M. Parkash, IR study of Pb–Sr titanate borosilicate glasses, Bull. Mater. Sci. 33 (2) (2010) 145–148.
[21] Y.I. Belyiand, N.A. Minakova, IR study of Pb–Sr titanate borosilicate glasses, Glass Ceram. 62 (2005) 337–340.